Colloids and Surfaces A: Physicochem. Eng. Aspects xxx (2014) xxx–xxx

Contents lists available at ScienceDirect

Colloids and Surfaces A: Physicochemical and Engineering Aspects

journal homepage: www.elsevier.com/locate/colsurfa

Membrane interaction of a new synthetic antimicrobial lipopeptide sp-85 with broad spectrum activity

Ariadna Grau-Campistany[a,b], Montserrat Pujol[a], Ana M. Marqués[c], Ángeles Manresa[c], Francesc Rabanal[b], Yolanda Cajal[a,*]

[a] Department of Physical Chemistry, Faculty of Pharmacy, University of Barcelona, Joan XXIII s/n, 08028 Barcelona, Spain
[b] Department of Organic Chemistry, Faculty of Chemistry, University of Barcelona, Martí i Franquès 1, 08028 Barcelona, Spain
[c] Laboratory of Microbiology, Faculty of Pharmacy, University of Barcelona, Joan XXIII s/n, 08028 Barcelona, Spain

HIGHLIGHTS

- Sp-85 is a new synthetic antibiotic lipopeptide with broad spectrum activity.
- Pressure–area curves of mixed monolayers show non-ideal mixing.
- Binding to anionic liposomes results in fusion and leakage of aqueous contents.
- TEM images of antibiotic-exposed bacteria show damaged membranes.
- A mechanism of action based on bacterial membrane destabilization is proposed.

GRAPHICAL ABSTRACT

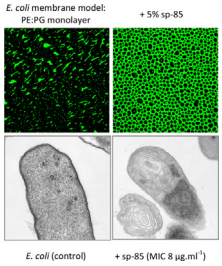

ARTICLE INFO

Article history:
Received 15 July 2014
Received in revised form 23 October 2014
Accepted 31 October 2014
Available online xxx

Keywords:
Antimicrobial peptide
Lipid–peptide interaction
Polymyxin B analogs
Model membrane
Langmuir monolayer
Liposomes

ABSTRACT

Antimicrobial peptides offer a new class of therapeutic agents to which bacteria may not be able to develop genetic resistance, since their main activity is in the lipid component of the bacterial cell membrane. We have developed a series of synthetic cationic cyclic lipopeptides based on natural polymyxin, and in this work we explore the interaction of sp-85, an analog that contains a C12 fatty acid at the N-terminus and two residues of arginine. This analog has been selected from its broad spectrum antibacterial activity in the micromolar range, and it has a disruptive action on the cytoplasmic membrane of bacteria, as demonstrated by TEM. In order to obtain information on the interaction of this analog with membrane lipids, we have obtained thermodynamic parameters from mixed monolayers prepared with POPG and POPE/POPG (molar ratio 6:4), as models of Gram positive and Gram negative bacteria, respectively. Langmuir–Blodgett films have been extracted on glass plates and observed by confocal microscopy, and images are consistent with a strong destabilizing effect on the membrane organization induced by sp-85. The effect of sp-85 on the membrane is confirmed with unilamelar lipid vesicles of the same composition, where biophysical experiments based on fluorescence are indicative of membrane fusion and permeabilization starting at very low concentrations of peptide and only if anionic lipids are present. Overall, results described here provide strong evidence that the mode of action of sp-85 is the alteration of the bacterial membrane permeability barrier.

1. Introduction

For the last decades antimicrobial resistance has been a growing threat to the effective treatment of an ever-increasing range

* Corresponding author. Tel.: +34 34024553.
E-mail address: ycajal@ub.edu (Y. Cajal).

http://dx.doi.org/10.1016/j.colsurfa.2014.10.062
0927-7757/

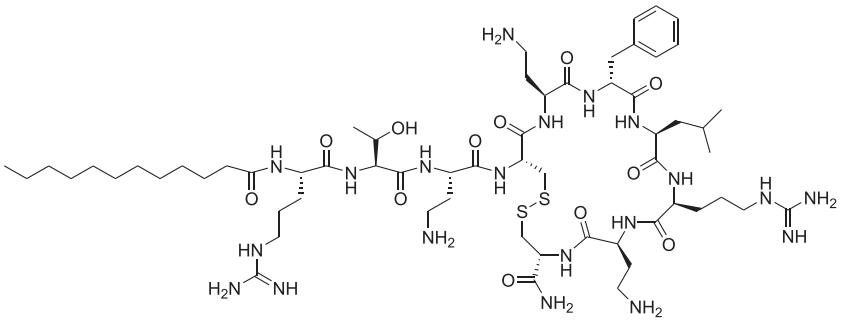

Fig. 1. Structure of sp-85, a synthetic decapeptide antibiotic formed by a (i) 7-member ring with 3 positive charges due to two 1,3-diaminobutyric acid (Dab) and one arginine (Arg) residues, and a hydrophobic segment (D-Phe-Leu), and (ii) a linear N-terminal region of 3 aminoacids with two positive charges (Dab and Arg), and a C12 fatty acid.

of bacterial infections, and it is now a complex public health challenge [1]. Some factors that have contributed to the development of resistance to current antibiotics include inappropriate use, such as the overuse of powerful, broad-spectrum antibiotics, the presence of antibiotics in the food/livestock industry, and the inclusion of antimicrobials in household products [2]. The World Health Organization recognizes antimicrobial resistance as one of the three greatest threats to human health [3]. However, the antimicrobial pipeline remains unacceptably lean, in fact, the ESKAPE pathogens (*Enterococcus faecium*, *Staphylococcus aureus*, *Klebsiella pneumoniae*, *Acinetobacter baumannii*, *Pseudomonas aeruginosa* and *Enterobacter sp*) have outpaced the drug discovery process [4,5]. This lack of new antimicrobials to replace those that become ineffective brings added urgency to the need to protect the efficacy of existing drugs. In the last few years there has been a resurgence of old antibiotics, and specially polymyxins discovered in the 1940s [6], as drugs of last resort for the treatment of infections caused by multi-drug resistant Gram-negative pathogens, despite their toxicity (nephro- and neurotoxicity) and the lack of clinical efficacy data [7,8]. Polymyxins belong to the class of antimicrobial peptides (AMPs), a class of antibiotics that have attracted great interest in the last few years because they rarely spur the development of resistant organisms. AMPs are a diverse group of molecules that share a few common features, the most important is that their main target is the lipid bilayer itself, and in consequence to develop genetic resistance is very costly for bacteria. AMPs are natural weapons produced by a variety of organisms, from single-celled microbes to vertebrates [9]. To date more than 2000 have been identified in nature and they are listed in the Antimicrobial Peptide Database (http://aps.unmc.edu/AP/main.php). They are very diverse in their sequences, length (generally short) and structures (some of them are linear while others are cyclic sometimes due to disulfide bridges, with a variety of secondary structures), but they adopt an amphipathic conformation that allows them to interact and disrupt selectively the negatively charged microbial membranes. No single mechanism can be defined for all AMPs, but despite these differences it can be concluded that they act mainly by binding to membranes and kill bacteria by disrupting membrane packing and organization, causing defects in the membrane with the consequent dissipation of transmembrane potential and leakage of important cellular contents [10–12]. In the case of PxB as well as cecropin and other AMPs, the proposed mechanism of action is based on the formation of periplasmic membrane contacts between outer and inner membranes. According to this model, once in the periplasmic space PxB forms contacts between the two enclosed phospholipid interfaces and promotes a fast exchange of certain phospholipids. The resulting changes in the membrane lipid composition trigger an osmotic imbalance that leads to bacterial stasis and cell death [13–15]. Sp-85 is a synthetic lipopetide that belongs to a family of more than 100 derivatives obtained by rational design based on the structure of natural antibiotic PxB [16–18]. The structure (Fig. 1) maintains the characteristics of PxB that are important for antibacterial activity, such as a cyclic nature, an overall positive charge, and an amphipathic structure, with two hydrophobic domains: a fatty acid in the N-terminus and two hydrophobic aminoacids in position 6–7 of the cycle. In this analog, some of the natural Dab residues of PxB have been substituted by Arg, another basic and positively charged aminoacid that is known to interact more strongly with the anionic membranes due to the particular properties of the guanidine group, providing arginine with strong bidentate cationic character and hydrogen-bond forming properties [19]. This allows arginine to form cation–π interactions that make insertion into the hydrophobic core of the bilayer energetically more favorable [20]. Herein we present biophysical studies to understand the membrane disruption mechanism for sp-85 using monolayers and bilayers as bacterial membrane models. Gram positive cytoplasmic membrane is modeled with POPG, whereas the Gram negative membrane is best mimicked with a binary mixture of POPE:POPG (molar ratio 6:4) [21]. Eukaryotic membranes tend to be neutral, and are modeled with zwitterionic POPC. Results are discussed in the light of the antibacterial activity of sp-85 on representative Gram positive and Gram negative bacteria and with its hemolytic activity *in vitro*.

2. Experimental

2.1. Chemicals

Phospholipids: 1-palmitoyl-2-oleoyl-glycero-*sn*- glycero-3-phospho-(1′-*rac*-glycerol) (POPG), 1,2-dipalmitoyl-*sn*-glycero-3-phospho-(1′-*rac*-glycerol) (DPPG), 1-palmitoyl-2-oleoyl-*sn*-glycero-3-phosphoethanolamine (POPE), 1,2-dipalmitoyl-*sn*-glycero-3-phosphoethanolamine (DPPE), and 1-palmitoyl-2-oleoyl-*sn*-glycero-3-phosphocholine (POPC) were from Avanti Polar Lipids (Alabaster, Ala). Fluorescently labeled phospholipids and probes: 1-oleoyl-2-[12-[(7-nitro-2-1,3-benzoxadiazol-4-yl)amino] dodecanoyl]-*sn*-glycero-3-[phospho-*rac*-(1-glycerol)] (NBD-PG), 1-hexadecanoyl-2-(1-pyrenedecanoyl) glycero-*sn*-3-phospho-(1′-*rac*-glycerol) (pyPG), 1-hexadecanoyl-2-(1-pyrenedecanoyl) glycero-*sn*-3-phosphocholine (pyPC), ANTS, 1-aminonapthalene-3,6,8-trisulfonic acid, and DPX, *N*,*N*′-*p*-xylenebis(pyridinium bromide) were purchased from Invitrogen Molecular Probes (Eugene, OR). *N*-fluorenylmethoxycarbonyl (Fmoc)-protected amino acids were purchased from Bachem (Bubendorf, Switzerland) and Fluka (Buchs, Switzerland). Chemical reagents *N*,*N*-diisopropylcarbodiimide (DIPCDI), *N*-hydroxybenzotriazole (HOBt), trifluoroacetic acid (TFA) (BioChemika quality) as well as dodecanoic acid were also from Fluka (Buchs, Switzerland). Rink amide resin was purchased from Novabiochem (Läufelfingen, Switzerland). Chloroform and methanol (HPLC grade, Fisher Scientific CO) were used as the

Please cite this article in press as: A. Grau-Campistany, et al., Membrane interaction of a new synthetic antimicrobial lipopeptide sp-85 with broad spectrum activity, Colloids Surf. A: Physicochem. Eng. Aspects (2014), http://dx.doi.org/10.1016/j.colsurfa.2014.10.062

spreading solvent for all lipids. Trizma base (Tris) was purchased from Sigma–Aldrich (St Louis, MO). Water was doubly distilled and deionized (Milli-Q system, Millipore Corp.).

2.2. Peptide synthesis and purification

Peptide synthesis was performed manually following standard Fmoc/^{t}Bu procedures using DIPCDI/HOBt activation on a Rink amide resin [22]. Once the sequence was assembled, cleavage of the peptide from the resin was carried out by acidolysis with TFA:triisopropylsilane:water (95:3:2, v/v/v) for 90 min. TFA was removed with N_2 stream and the oily residue was treated with dry diethyl ether to obtain the peptide precipitate. The solid peptide was isolated by centrifugation. This process was repeated three times. The homogeneity of peptide crude was assessed by analytical HPLC using Nucleosil C18 reverse phase columns (4 × 250 mm, 5 μm of particle diameter and 120 Å porous size). Elution was carried out at 1 ml min^{-1} flow with mixtures of H_2O – 0.045% TFA and acetonitrile – 0.036% TFA and UV detection at 220 nm. Sp-85 crude was purified by preparative HPLC on a Waters Delta Prep 3000 system using a Phenomenex C18 (2) column (250 × 10 mm, 5 μm) eluted with H_2O–acetonitrile – 0.1% TFA gradient mixtures and UV detection at 220 nm. Cyclization through disulfide bond was carried out in 100 mM ammonium bicarbonate aqueous solutions with a pH adjusted to 10 by addition of aqueous concentrated ammonia (32%). Final purity was greater than 95%. The synthetized lipopeptide was characterized by amino acid analysis with a Beckman 6300 analyzer and by MALDI-TOF with a Bruker model Biflex III.

2.3. Pressure–area compression isotherms

Pressure–area curves of monolayers were performed with a fully automated monolayer system (NIMA technology, Coventry, England) equipped with a pressure sensor PS4 and a software trough, enclosed in a Plexiglas box to reduce surface contamination. The surface pressure (π) of the lipid monolayer was measured by the Wilhelmy method, with a sand-blasted platinum plate connected to an electrobalance. The PTFE trough (surface area 525 cm^2, volume 250 cm^3) and the plate were thoroughly cleaned before each run with hot water to avoid carry-over of lipid or peptide. Lipid solution was prepared by dissolving the lipid or lipid mixture in chloroform/methanol (9:1, v/v) to a concentration in lipid of 1.3 mM. Peptide solution was prepared by first dissolving the lyophilized powder in a minimal amount (<5%) of dimethylsulfoxide (DMSO) and then diluting to a final concentration of 1.3 mM with chloroform/methanol (2:1, v/v). Monolayers were formed by applying small drops of the spreading solutions (lipid, peptide, or binary mixtures) on the 10 mM Tris buffer subphase (pH 8.0) with a microsyringe (Hamilton Co., Reno, NV). After 10 min, allowing for solvent evaporation and stabilization of the monolayers, they were continuously compressed (symmetrical compression) with an area reduction rate of 20 cm^2 min^{-1}. The films were compressed up to their collapse pressure. Standard deviation was typically ±0.5%. Experiments were done at 24 °C.

2.4. Morphology of LB films

At a given surface pressure, Langmuir–Blodgett films (LB) of the chosen monolayers doped with 1% NBD-PG were obtained by transferring onto Menzel-Gläser cover glass plates (20 × 20 mm) by vertically raising the plate through the air-water interface at a rate of 5 mm min^{-1}. The surface pressure was kept constant at the selected value with a feedback system, and extraction was started when a stable baseline was obtained for at least 15 min. The cover glass had been previously half-dipped into the subphase before monolayer deposition. The subphase was unbuffered and salt free, to avoid formation of crystals on the samples. The LB films were observed in a confocal fluorescence microscope (Leica, Germany) equipped with the appropriate filters to allow for observation of NBD fluorescence (excitation 480 nm, emission 527 nm) at a magnification of 60×.

2.5. Lipid vesicles

Unilamelar vesicles of POPG, POPE/POPG (6:4) or POPC, alone or with the fluorescently labeled phospholipids (pyPG or pyPC) were prepared by evaporation of a mixture of the lipids and probes in chloroform/methanol (2:1 v/v). The dried film was hydrated for a final lipid concentration of 10 mM, and then sonicated in a bath type sonicator (Lab Supplies, Hickesville, NY, Model G112SPIT) until a clear dispersion was obtained (typically 2–4 min). For the ANTS/DPX fusion assay, the dried lipid films were dispersed in 12.5 mM ANTS, 45 mM DPX and 10 mM Tris buffer at pH 8.0 and subjected to 10 freeze–thaw cycles prior to extrusion 10 times through a 0.1 μm polycarbonate membrane at 250 psi N_2 pressure (LIPEX, Northern Lipids Inc.). The unencapsulated material was separated by gel-filtration on a Sephadex G-50 column eluted with 10 mM Tris buffer and 80 mM NaCl. Osmolarities were adjusted with NaCl and measured in an osmometer (3320 Osmometer, Advanced Instruments Inc.). Lipid phosphorus was determined by the Stewart-Marshall assay. These vesicles were used within 10 h. Vesicle size was measured by dynamic light scattering with a Malvern II-C autosizer, typically obtaining a mean diameter of 80 nm and 105 nm for sonicated and extruded respectively, and a narrow size distribution (polydispersity <0.1).

2.6. Fluorescence assay for lipid mixing

The mixing of lipids between membranes induced by the lipopeptide was determined using small unilamelar vesicles, as described in detail elsewhere [23]. Unilamelar vesicles of POPG, POPE/POPG (6:4) or POPC, alone or with 30% of the fluorescently labeled phospholipids (pyPG or pyPC) were prepared by sonication, as described previously. Transfer of pyrene-labeled phospholipids as donor vesicles (0.83 μM) to an excess of unlabeled phospholipid vesicles (106 μM) as acceptors was measured. Emission from vesicles containing 30% pyrene-phospholipid is dominated by the excimer band at 480 nm, and the intensity of the monomer band, at 395 nm, increases as the probe is diluted due to exchange with excess unlabeled vesicles in contact. Experiments were carried out at 24 °C in 10 mM Tris buffer at pH 8.0 on a PTI QM4 spectrophotometer with constant stirring. Peptide was added from a stock solution 0.25 mM in water to the cuvette containing vesicles of the desired composition. Fluorescence emission was monitored at 395 nm (with excitation at 346 nm) corresponding to the monomer emission. The slit widths were kept at 2 nm each.

2.7. Dye leakage

Dequenching of co-encapsulated ANTS and DPX fluorescence resulting from dilution was measured to assess leakage of aqueous contents [24]. Fluorescence measurements were performed at 24 °C in 10 mM Tris buffer at pH 8.0 on a PTI QM4 spectrophotometer with constant stirring by setting the ANTS emission at 530 nm and the excitation at 350 nm. Peptide was added from a stock solution 0.25 mM in water to the cuvette containing vesicles of the desired composition (lipid concentration 115 μM). The percentage of leakage was determined from:

$$\% \text{ leakage} = [(F_t - F_0)/(F_{max} - F_0)] \times 100$$

Please cite this article in press as: A. Grau-Campistany, et al., Membrane interaction of a new synthetic antimicrobial lipopeptide sp-85 with broad spectrum activity, Colloids Surf. A: Physicochem. Eng. Aspects (2014), http://dx.doi.org/10.1016/j.colsurfa.2014.10.062

where F_0 corresponds to the fluorescence of the vesicles alone at time zero, F_{max} is the fluorescence value obtained after addition of Triton X-100 (10% v/v), to induce total leakage, and F_t is the fluorescence intensity after addition of the peptide.

2.8. Determination of antibacterial activity

The minimal inhibitory concentration (MIC) of the synthetic lipopeptides against *Escherichia coli* (ATTC 25922), *Pseudomonas aeruginosa* (ATCC 9027), *Staphylococcus aureus* (ATTC 29213) and *Enterococcus faecalis* (ATTC 29212) was determined by the broth microdilution method [25] in Mueller-Hinton broth (MHB) in 96-well polypropylene microtiter plates with a final concentration of 10^5 CFU/mL in each well. The MIC was determined as the lowest peptide concentration at which growth was completely inhibited after overnight incubation of the plates at 37 °C. Each determination was done by triplicate and with two controls, drug-free and microorganism-free.

2.9. Measurement of hemolytic activity

Hemolysis was determined according to [26]. Briefly, fresh rabbit red blood cells were washed three times with buffer (150 mN NaCl/5 mM Hepes, pH 7.3) by centrifugation at 3000 rpm 10 min, and finally resuspended in the same volume of buffer prior to use. This erythrocyte concentrate was diluted with 150 mM NaCl, 5 mM Hepes pH 7.3 buffer to obtain a suspension with $A_{540} = 1$. All operations were carried out at 4 °C. Aliquots of a peptide solution in buffer were added to 300 μl of the erythrocyte suspension, and samples were incubated at 37 °C for 1 h. Hemoglobin release was determined by measuring the absorbance at 540 nm after pelleting the membranes by centrifugation for 2 min in a bench microfuge (A_{sample}). As negative and positive controls, erythrocytes in buffer (A_{blank}) and in distilled water (A_{water}) were employed, respectively. The hemolysis percentage was calculated according to the equation:

$$\%\ \ hemolysis = 100 \times \left[\frac{A_{sample} - A_{blank}}{A_{water} - A_{blank}}\right]$$

2.10. Preparation of cells for TEM

An overnight culture (12–16 h) of *E. coli* (ATCC 25922) in TSB was grown at 37 °C and 500 μL were added in 50 mL of tryptone water (~10^8 bacteria ml^{-1}). The bacterial suspension was split into aliquots of 10 mL and treated with sp-85 at the MIC for 120 min at room temperature. Cells were collected by centrifugation (12,857 × *g*, 20 min). Samples were fixed with 2.5% glutaraldehyde in phosphate buffer for 2 h at 4 °C, washed with the same buffer and post fixed with 1% osmium tetroxide in buffer containing 0.8% potassium ferricyanide at 4 °C. The samples were then dehydrated for 1 h in acetone and infiltrated in a graded series of Epon resin (Ted pella, Inc., USA) during 2 days, and finally embedded in fresh Epon resin and polymerized at 60 °C during 48 h. Ultrathin sections were obtained using a Leica Ultracut UCT ultramicrotome (Leica, Vienna) and mounted on Formvar-coated copper grids. Sections were stained with 2% aqueous uranyl acetate and lead citrate and examined in a JEM-1010 electron microscope (Jeol, Japan).

3. Results and discussion

3.1. Antibacterial and hemolytic activities of sp-85

The MIC values of sp-85 and the related natural antibiotic polymyxin B (parental peptide used as control) against representative Gram positive and Gram negative bacteria are shown in Table 1. Polymyxin B is a very potent antibiotic against Gram negative bacteria, but it has no activity on Gram positives. The main reason for this selectivity has been proposed to be the particular mechanism of action of this lipopeptide, causing a selective mixing of lipids between outer and inner membranes of Gram negative bacteria, resulting in an osmotic imbalance that causes cell death [15]. Interestingly, our synthetic analog is less active against representative Gram negative bacteria, but it shows good activity in Gram positive bacteria, especially in *S. aureus*, with a MIC of 4 μM, and this implies a different mechanism of antimicrobial action.

Table 1
Antimicrobial activities of sp-85 and polymyxin B in Gram positive (*Staphylococcus aureus* and *Enterococcus faecalis*) and Gram negative (*Escherichia coli* and *Pseudomonas aeruginosa*) bacteria.

	MIC (μg ml^{-1})			
	S. aureus	*E. faecalis*	*E. coli*	*P. aeruginosa*
sp-85	4	8	8	16
PxB	> 32	>32	1	1

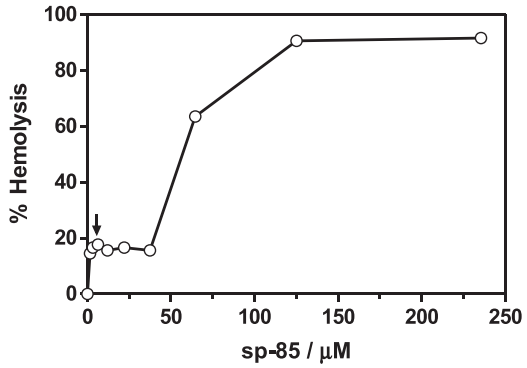

Fig. 2. Dependence of erythrocyte hemolysis on sp-85 concentration. Erythrocytes were incubated for 1 h at 37 °C at different peptide concentrations, and the amount of hemoglobin release was determined. The average MIC of sp-85 from results in Table 1 is indicated with an arrow. Data correspond to the average of three independent experiments (error <5%).

The dependence of hemolysis on the concentration of sp-85 after 1 h of incubation at 37 °C is shown in Fig. 2. A biphasic behavior is observed, with very low hemolysis below 40 μM, a concentration that is well above the MIC of this peptide, and a sharp increase at higher concentrations, reaching more than 90% at 125 μM.

3.2. Surface pressure–area isotherms

The π–A isotherms for pure phospholipids, pure peptide and the different mixtures on a 10 mM Tris pH 8.0 subphase are shown in Fig. 3. Molecular areas shown in this figure are calculated for the total number of spread molecules, both lipid and peptide. For each isotherm, the compressibility modulus (C_s^{-1}) was calculated as:

$$C_s^{-1} = -A(\delta\pi/\delta A)_T$$

This parameter is used to characterize the phase of a monolayer [27] considering that for a liquid expanded (LE) film, it ranges from 12.5 to 50 mN m^{-1} and for a liquid condensed phase (LC), values oscillate from 100 to 250 mN m^{-1}. Analyzing the isotherms of pure lipids, it can be noticed that monolayers with unsaturated oleic acid in position *sn*-2 (POPG or POPE/POPG) are more expanded that the corresponding monolayers of saturated lipids with the same headgroup composition, which is consistent with values in the literature for these lipid systems [28], and expected due to the higher degree of packing of saturated lipids. DPPG and DPPE form highly ordered monolayers due to the ability of both phospholipids to form

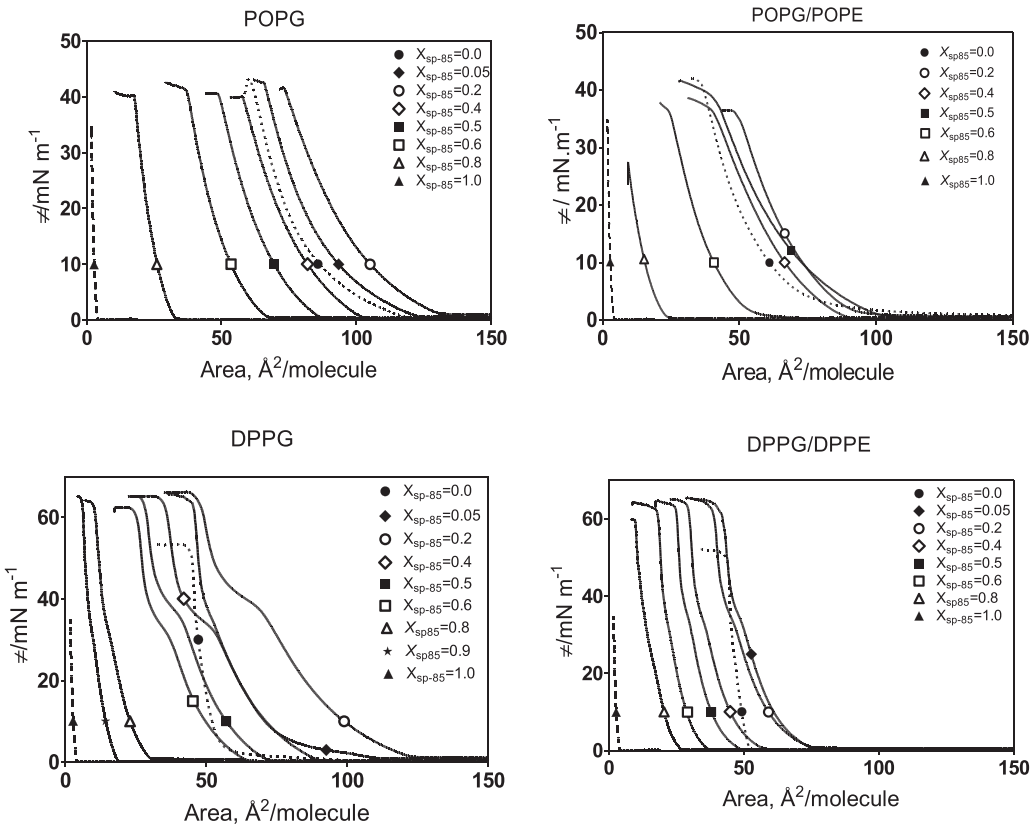

Fig. 3. Surface pressure–area isotherms for the investigated monolayers. Molar fraction of sp-85 is indicated as an *inset*.

intermolecular hydrogen bonds between the glycerol hydroxyl and the phosphate group in DPPG, and between ammonium and phosphate group in DPPE. According to C_s^{-1} calculations, POPG monolayer is in a LE phase up to 18 mN m^{-1}, and reaches the collapse without adopting the LC phase. In the case of saturated DPPG, above a surface pressure of 10 mN m^{-1} the monolayer adopts the LC phase, and is in a solid phase at high pressures (>35 mN m^{-1}), before reaching collapse at 55 mN m^{-1}. At 35 mN m^{-1} there is a change of the slope that indicates that during compression the phase transition from LC to solid-condensed occurs.

The presence of sp-85 has a strong effect on the lipid packing, with an increase in the molecular area that depends on the peptide concentration. In Fig. 4, the area per molecule values calculated from the isotherm registers in Fig. 3 are plotted as a function of the peptide mole fraction. Results show positive deviations from ideal mixing, that will correspond to a straight line according to the additivity rule, at all surface pressures. This suggests that the lipids and sp-85 are miscible and that they interact in such a way that the intrinsic area values of the individual components are changed. Similar results were obtained for polymyxin B in monolayers of *E. coli* lipid extract [29]. These positive deviations from ideal mixing occur in PG and PG/PE monolayers, both saturated and unsaturated, and are indicative of repulsive interactions between the components; interactions are less significant as the surface pressure increases and the film components are in a more condensed form. Analysis of the compressibility modulus also gives information of the effect of sp-85 in the lipid packing. Insertion in fluid POPG monolayers results in higher compressibility values, indicating an increase in lipid packing. For example, POPG at a surface pressure of 32 mN m^{-1} has a compressibility of 75 mN m^{-1}, compared to 100 mN m^{-1} in the presence of 0.2 mole fraction of sp-85 at the same surface pressure. In contrast, insertion of sp-85 into the densely packed DPPG results in a less condensed monolayer, with

Table 2
Excess Gibbs energy of mixing (kJ mol^{-1}) at 32 mN m^{-1} for the different lipid compositions, as a function of the mole fraction of sp-85.

X_{sp85}	POPG	POPG/POPE	DPPG	DPPG/DPPE
0.05	0.63	0.45	2.09	1.37
0.2	1.53	1.12	3.00	1.64
0.4	1.03	0.76	1.86	1.12
0.5	0.91	2.64	1.58	0.75
0.6	0.77	0.59	1.72	0.91
0.8	0.26	–	0.86	0.71

an important reduction of C_s^{-1} values, that are below 100 mN m^{-1} up to surface pressures of 35 mN m^{-1}, the surface pressure where the plateau occurs independently of the peptide concentration. The binary mixtures only adopt the LC phase at higher surface pressures, and they are very stable, with a collapse pressure well above that of the pure lipid (Fig. 3). Similar results are obtained for DPPE/DPPG (6:4) monolayers.

Further information on the interactions of sp-85 with the lipid systems are drawn from the analysis of the excess free energy of mixing values, calculated according to:

$$\Delta G_m^E = \int_{\pi\to 0}^{\pi} A_{12}\,d\pi - X_1 \int_{\pi\to 0}^{\pi} A_1\,d\pi - X_2 \int_{\pi\to 0}^{\pi} A_2\,d\pi$$

where A_{12} is the mean molecular area in the mixed film, A_1 and A_2 are the molecular areas of the two pure components, all integrated between 0 mN m^{-1} and different pressure limits, and X_1 and X_2 are the molar fractions of monolayer components (lipid and peptide). In Table 2, excess free energy of mixing values at 32 mN m^{-1} are shown for all four lipid monolayer compositions and at different peptide mole fractions. This pressure is of special interest because it is known that the properties of Langmuir monolayers at the surface

Please cite this article in press as: A. Grau-Campistany, et al., Membrane interaction of a new synthetic antimicrobial lipopeptide sp-85 with broad spectrum activity, Colloids Surf. A: Physicochem. Eng. Aspects (2014), http://dx.doi.org/10.1016/j.colsurfa.2014.10.062

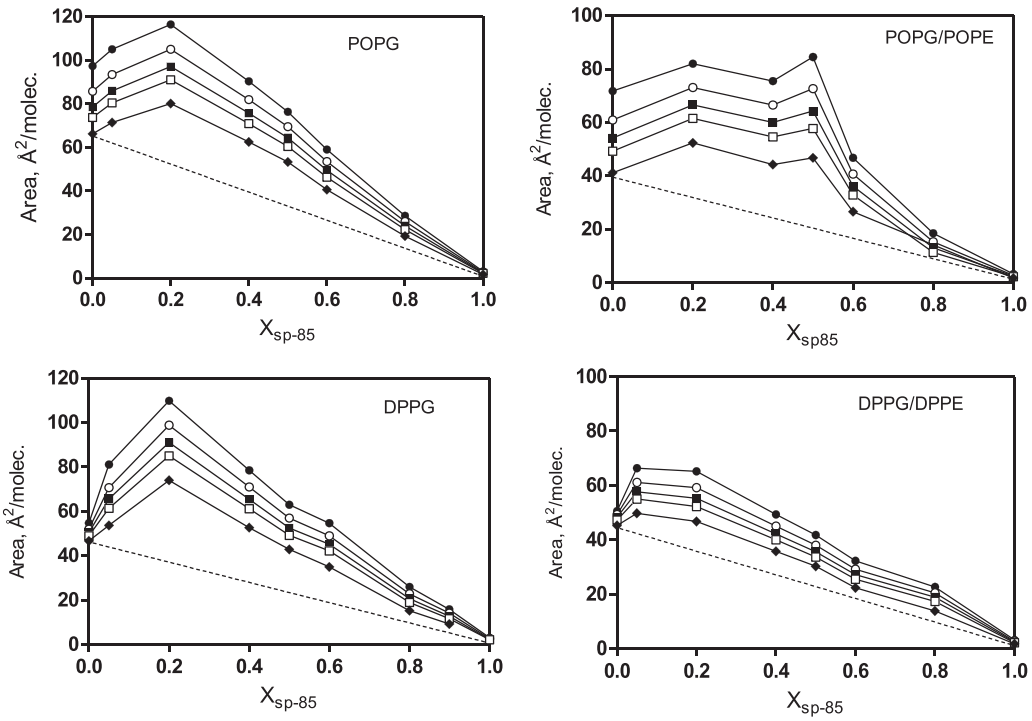

Fig. 4. Molecular area analysis. The mean molecular area of the different lipid/sp-85 monolayers at various surface pressures (mN m^{-1}): (●) 5, (○) 10, (■) 15, (□) 20 and (♦) 32.

pressure between 30 and 35 mN m^{-1} can be analyzed in the context of the properties of a biological membrane [30]. All ΔG^E values are positive, a fact that provides key information about the behavior of the lipid-peptide interaction. Positive values of ΔG^E indicate that the interaction between the two components, lipid and peptide in this case, is not energetically favored compared to an ideal mixture, where it is assumed that no difference exists in the interaction potentials when a molecule interacts with another molecule of the same molecular species or with a different one. It is generally accepted that positive values of ΔG^E are indicative of a preferential interaction between molecules of the same kind, resulting in the formation of oligomers or aggregates. As seen in Table 2, in

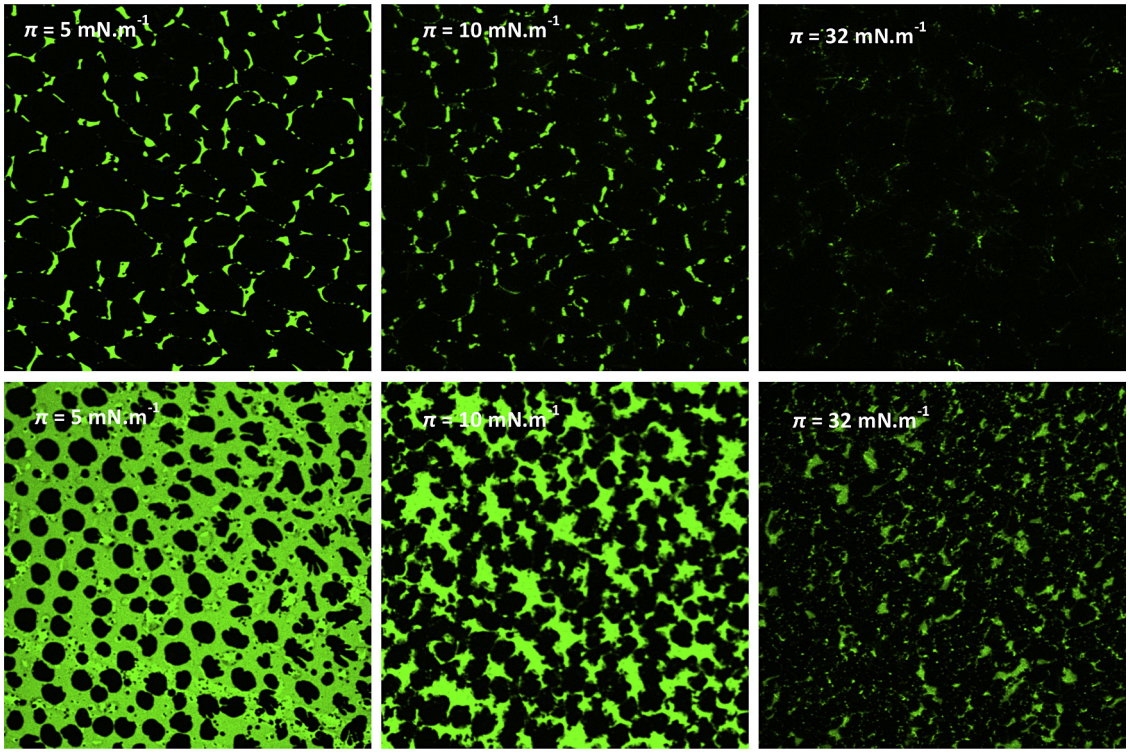

Fig. 5. Domain morphology of a DPPG LB monolayer on a water subphase at 24 °C at different surface pressures in the absence (top) or in the presence of 5% sp-85 (bottom). LB films doped with 1% NBD-PG were extracted on glass plates and observed with a confocal microscope. Image size is 116.40 μm × 116.40 μm.

Please cite this article in press as: A. Grau-Campistany, et al., Membrane interaction of a new synthetic antimicrobial lipopeptide sp-85 with broad spectrum activity, Colloids Surf. A: Physicochem. Eng. Aspects (2014), http://dx.doi.org/10.1016/j.colsurfa.2014.10.062

some cases ΔG^E values are very high even at very low concentrations of peptide in the membrane. For example, for $X_{sp\text{-}85}$ = 0.05 in DPPG, ΔG^E is 2090 J mol^{-1}, an elevated value that can be attributed to the formation of peptide oligomers or clusters in the dominant lipid phase. Formation of oligomers has been suggested for PxB in anionic vesicles [31].

3.3. Morphological changes in the lipid monolayers induced by sp-85

To complete the analysis of the isotherms, the properties of the monolayers formed by the investigated phospholipids mixed with sp-85 were studied by observation of extracted LB films doped with 1% NBD-PG and formed on a water subphase by confocal fluorescence microscopy. This technique allows visualizing the morphological changes of the monolayer due to sp-85 insertion on the basis of segregation of the NBD probe from the ordered condensed domains (LC and solid) due to steric hindrance. The less ordered phases (gas and LE) are bright as a result of dye partitioning. Results shown here correspond to the monolayers of saturated lipids, because the POPG and POPG/POPE films do not adopt the LC phase upon compression, and therefore no condensed domains can be seen visually and images correspond to a homogeneous LE film (not shown). Control experiments show that the presence of the NBD-labeled phospholipid does not modify the π–area curves.

The images corresponding to a pure DPPG monolayer extracted at three different surface pressures are shown in Fig. 5 (top), and the C_s^{-1} of the corresponding isotherm is in Fig. 6. At 5 mN m^{-1}, C_s^{-1} is 56 mN m^{-1}, indicative of a maximally condensed LE state, with abundant dark domains in the microscopy image; upon compressing to 10 mN m^{-1} the image shows an increase in area occupied by dark compressed domains, as expected given that the lipid is mostly in the LC phase (C_s^{-1} = 138 mN m^{-1}). Finally, at 32 mN m^{-1} one can see an almost homogeneous dark layer as the monolayer adopts the solid phase (C_s^{-1} = 270 mN m^{-1}). Addition of 5% sp-85 has a strong effect on the DPPG lipid monolayer, as already seen in Figs. 3 and 4, with an important expansion of the area per molecule and a positive excess free energy of mixing. C_s^{-1} calculations (Fig. 6) show a less condensed monolayer, as also corroborated in the fluorescence microscopy images (Fig. 5 *bottom*), where the ratio of dark to bright regions is reduced. At π = 5 mN m^{-1} (C_s^{-1} = 26 mN m^{-1} indicative of a monolayer in the LE phase), images show small domains of dark condensed phase in a bright matrix of fluid LE phase. At π = 10 mN m^{-1}, the area occupied by the condensed phase domains increases, but there is still an important percentage of expanded phase compared to the pure lipid. The lipopeptide also induces some fuzziness at the domain boundaries, that are not as regular and sharp as in low pressures. This suggests that the phase boundaries could be the preferred locations for peptide insertion. Finally, even at high pressures the monolayer is significantly less condensed that the pure lipid one, in agreement with a much lower compressibility factor (C_s^{-1} = 94 mN m^{-1} at π = 32 mN m^{-1}). This effect of sp-85 on DPPG is not unique, and for example the Alzheimer Aβ40 peptide also induces similar domain morphology changes [32].

Similar results are obtained for monolayers of the binary mixture (DPPE/DPPG 6:4). C_s^{-1} calculations (Fig. 6) clearly indicate that in the presence of DPPE the monolayer is more condensed that pure DPPG. The reason is the favorable interactions between these two phospholipids [28]. In the mixed monolayers, DPPE intercalates between DPPG molecules to reduce electrostatic repulsion, and in addition, the positively charged ammonium of PE are more strongly attracted to anionic PG than to zwitterionic PE, resulting in easier formation of hydrogen bonds compared to the pure lipid monolayers. As seen in Fig. 7, at a lateral pressure of

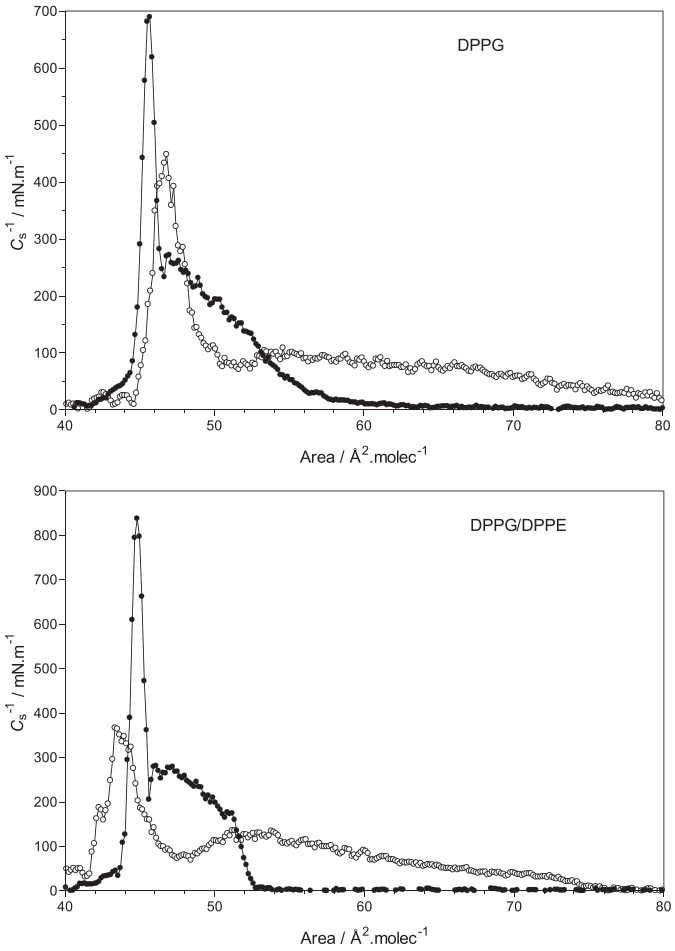

Fig. 6. Compressibility modulus (C_s^{-1}) analysis of isotherms for the lipid/sp-85 mixed monolayers with $X_{sp\text{-}85}$ = 0.05. These are the monolayers extracted as LB films for the morphological analysis. Closed circles: pure lipid; open circles: $X_{sp\text{-}85}$ = 0.05.

5 mN m^{-1}, the monolayer is mostly in the liquid condensed phase (C_s^{-1} = 164 mN m^{-1}), and increasing the pressure to 10 mN m^{-1} shows an even larger proportion of dark domains. At 32 mN m^{-1}, a change in slope in the compression isotherm (Fig. 3, more clearly seen as a minimum in compressibility modulus in Fig. 6) indicates the LC to S phase transition, and the image in Fig. 7 is compatible with a highly dense solid phase. Addition of 5% sp-85 changes the morphology of the DPPE/DPPG monolayer at all surface pressures, as illustrated in Fig. 7 (bottom). At low pressure (5 mN m^{-1}), the lower C_s^{-1} (49 mN m^{-1}) agrees with a less packed LE monolayer induced by the lipopeptide, in accordance with the fluorescence image where small condensed domains quite homogeneous in size and shape appear in a highly fluorescent background of more fluid LE phase. These domains are more abundant upon compression to higher pressures, and at 32 mN m^{-1}, the membrane equivalence pressure, they are still visible and occupy most of the available surface, although according to C_s^{-1} at this pressure (85 mN m^{-1}), the monolayer does not adopt the LC phase. Phase transition takes place at higher pressures, as indicated by the plateau at 35 mN m^{-1} in the compression isotherm and in the minimum C_s^{-1} (Fig. 6).

3.4. Membrane destabilization induced by sp-85

Unilamelar vesicles of phospholipids have long served as models for biological membranes, and provide useful information on peptide–lipid interactions that complement the information obtained from monolayers. Many antimicrobial peptides act on the

Please cite this article in press as: A. Grau-Campistany, et al., Membrane interaction of a new synthetic antimicrobial lipopeptide sp-85 with broad spectrum activity, Colloids Surf. A: Physicochem. Eng. Aspects (2014), http://dx.doi.org/10.1016/j.colsurfa.2014.10.062

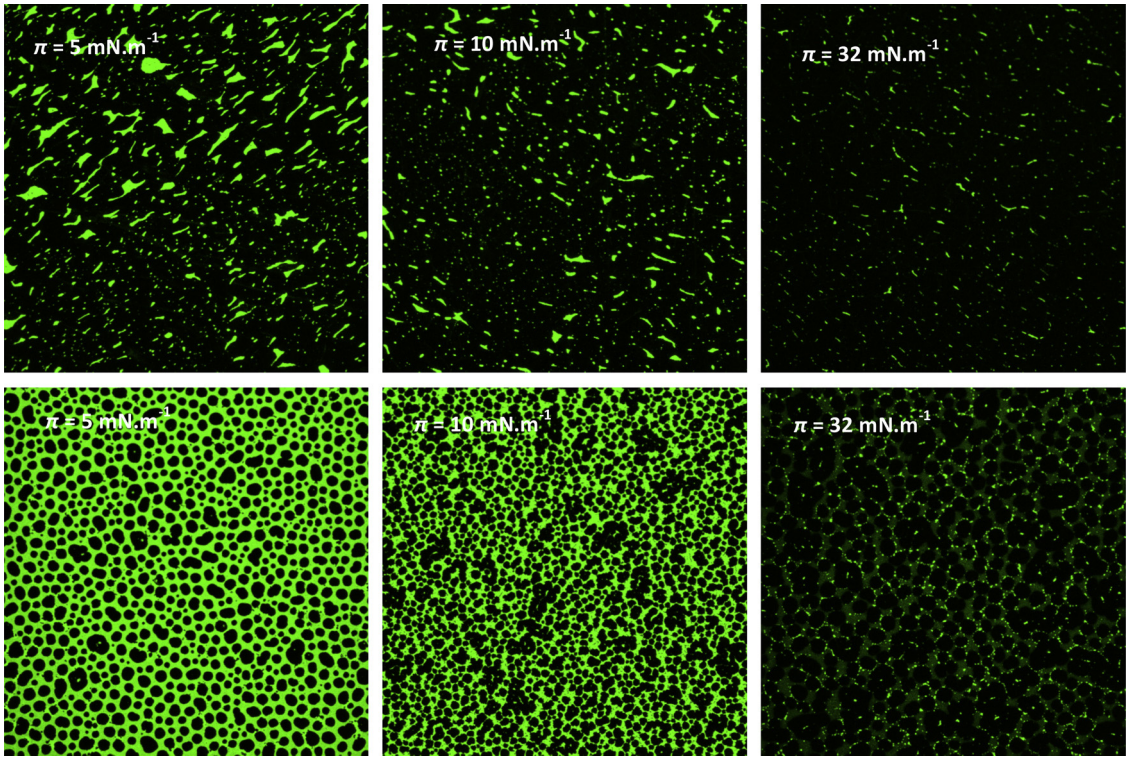

Fig. 7. Domain morphology of a DPPE/DPPG (6:4) LB monolayer on a water subphase at different surface pressures in the absence (top) or in the presence of 5% sp-85 (bottom). Other conditions as in Fig. 5.

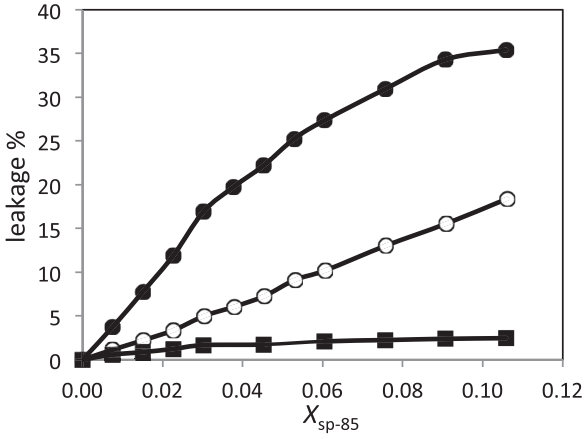

Fig. 8. Peptide induced leakage from liposomes of POPE/POPG (6:4) (●), POPG (○), or POPC (■). Increasing concentrations of sp-85 were added to a solution of liposomes (lipid concentration 115 μM) co-encapsulating ANTS (12.5 mM) and DPX (45 mM), and leakage was monitored as the increase in fluorescence intensity due to ANTS. Excitation 350 nm, emission 530 nm.

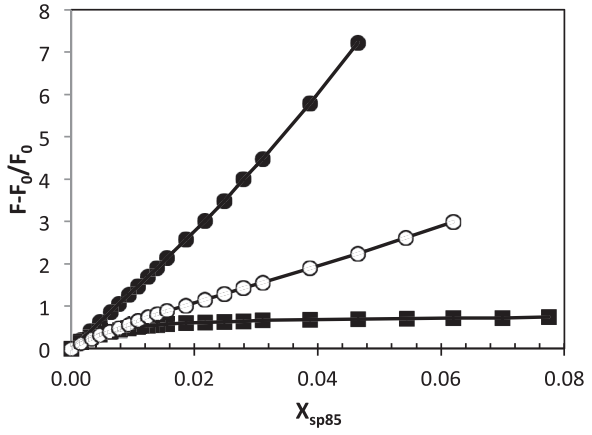

Fig. 9. Increase in fluorescence intensity of pyrene monomer as a function of lipopeptide added to vesicles of different composition: POPE/POPG (6:4) (●), POPG (○), or POPC (■). Vesicles are a mixture of POPG/pyPG or POPE/pyPG (0.83 μM) and unlabeled vesicles of the same composition (106 μM) in 10 mM Tris pH 8.0. Excitation 346 nm, emission 395 nm.

bacterial membrane, disrupting its organization in different ways [33], ultimately causing loss of membrane potential, cessation of macromolecule synthesis and cell death [9,10]. We have determined the ability of sp-85 to induce membrane fusion and leakage of aqueous contents from unilamelar vesicles of the same compositions used in the monolayers: POPG and POPE:POPG (6:4), as models of the bacterial membrane of representative Gram positive and Gram negative cytoplasmic membrane, respectively. In addition, POPC vesicles are used to mimic the composition of the eukaryotic membrane, rich in zwitterionic phosphatidylcholine. The first important observation is that sp-85 has a strong destabilizing effect on anionic membranes, both POPG and the binary mixture, but it has almost no effect on zwitterionic POPC (Figs. 8 and 9).

The ability of sp-85 to induce permeabilization of the bacterial membrane-mimicking anionic vesicles was determined measuring the concentration-dependent leakage of aqueous fluorescent dye ANTS co-encapsulated with the quencher molecule DPX. As shown in Fig. 8, leakage from POPE:POPG(6:4) vesicles is more extensive than from POPG liposomes for the same peptide concentration. If we consider a MIC value of 8 μg ml^{-1} (or 6 μM) for sp-85 as a representative activity for this peptide (Table 2), the induced leakage at this concentration is 9% and 25% for POPG and POPE/POPG respectively, whereas in POPC is less that 1%. The observed increase in ANTS fluorescence signal from anionic vesicles exposed to

Please cite this article in press as: A. Grau-Campistany, et al., Membrane interaction of a new synthetic antimicrobial lipopeptide sp-85 with broad spectrum activity, Colloids Surf. A: Physicochem. Eng. Aspects (2014), http://dx.doi.org/10.1016/j.colsurfa.2014.10.062

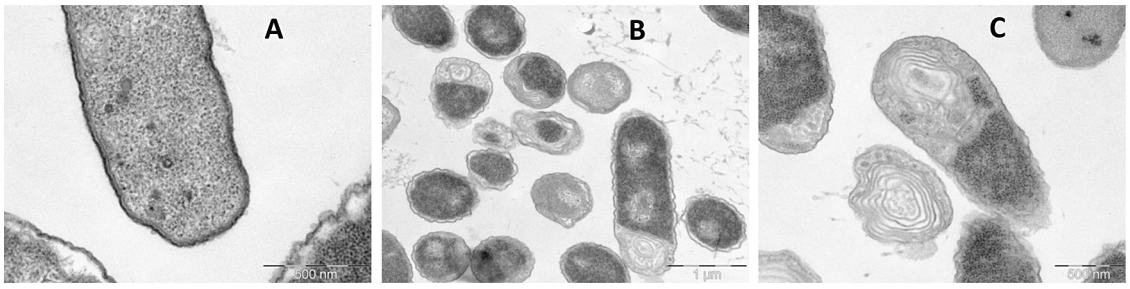

Fig. 10. TEM micrographs of *E. coli* cells treated with sp-85 at its MIC (8 μg ml^{-1}) for 2 h (A) Untreated cells with smooth, intact surfaces. (B, C) Sp-85-induced formation of membranous inclusions and alteration and breakage of the cell wall. Leakage of the inner mass of the cell is also visible.

sp-85 is related to an increase in particle size according to 90° light scattering experiments (not shown), thus suggesting aggregation of vesicles and ruling out the possibility of a detergent or lytic effect on the membrane. Pyrene-based experiments were used to determine the possibility of lipid mixing between vesicles induced by sp-85. Results shown in Fig. 9 clearly show that sp-85 causes the mixing of anionic lipids between vesicles of POPG and also of POPE/POPG (6:4), in good agreement with the leakage experiments, and suggesting that membrane fusion takes place starting at low concentrations of peptide. Lipid mixing does not take place in POPC vesicles, even at high concentrations of sp-85. Aggregation and fusion of anionic vesicles is not uncommon for antimicrobial peptides acting on the bacterial membrane, and in some cases it has been demonstrated that the effect is enhanced by the presence of POPE, for example in the case of antimicrobial peptide pheromone plantaricin A [34] and the Ca^{+2}-dependent lipopeptide antibiotic MX-2401 [35].

3.5. Ultrastructural effects of sp-85 on Escherichia coli

Untreated cells of *E. coli* in standard tryptone water medium show a normal cell shape with an undamaged structure of the inner membrane and an intact, slightly waved outer membrane (Fig. 10A). After 2 h of incubation with sp-85 at the MIC (8 μg/mL), remarkable modifications on the bacterial cell membrane and in the cytoplasm are seen indicating peptide-induced damage. TEM images show the disappearance of the periplasm due to the severe damage of the cytoplasm membrane and numerous spherical double-layered membranous inclusions, most prominent at the periphery of the cells, and a damaged cell wall with cracks and leakage of cellular components (Fig. 10B and C). Other effects include alterations in DNA region. Bacterial death is confirmed by plate count, therefore it is clear that the observed over-production of membrane has an effect on cell viability.

4. Conclusions

Pathogen resistance to more than one class of antibiotics, both in hospital and community settings, is a global concern that continues to escalate. Lipopeptides are a promising class of antibacterial agents because they do not act *via* a stereospecific protein receptor mediated mechanism, but rather target the fundamental difference in membrane composition between the host and the pathogens. This implies that bacteria are less able to develop resistance against this class of antibiotics, since changing the membrane composition is not a metabolically favorable process. Not a single mechanism of action can be defined for all peptides, and in many cases the molecular basis of the antimicrobial action on the membrane is not clear. In this work we have studied the membrane interaction/disruption mechanism for the antimicrobial lipopeptide sp-85, a synthetic analog of natural PxB. The broad spectrum of activity of sp-85, with MIC values in the micromolar region for both Gram positive and Gram negative bacteria, makes it an attractive antibiotic candidate. Langmuir monolayers, LB films and liposomes of different composition were selected as membrane models. Gram negative membranes are mostly composed of two main phospholipids: zwitterionic PE and anionic PG, and Gram positive bacteria have a membrane that is almost entirely formed by anionic phospholipids, such as PG [21]. The outer leaflet of mammalian cell membranes is mainly composed of PC, which is charge-neutral at physiological pH. These phospholipids have been used in biophysical studies to study the interaction of a variety of AMPs with the lipid membrane, for example synthetic lipopeptides MX-2401 [35] and MSI-843 [36], the short cationic peptide MP196 [37], or the human antimicrobial peptide LL-37 [38].

Monolayers are membrane models with important advantages over lipid vesicles; for example, with the monolayer system several parameters, such as the nature and packing of the lipid molecules, the composition of the subphase, and the temperature, can be chosen without limitation [39]. In addition, monolayers are bidimensional model membranes with a planar geometry where the lipid molecules have a defined orientation, and are very suitable for thermodynamic analysis. We have previously shown that PxB inserts into anionic monolayers of *E. coli* lipid extracts, expands de monolayer to higher areas per molecule and has a non-ideal mixing behavior with the lipids, with positive excess Gibbs energy values [29]. In the work described here we have demonstrated that sp-85 behaves in a very similar way, changing the spreading properties of anionic monolayers of POPG and POPE:POPG (6:4). Calculations of the excess area, a parameter that is defined as the difference between the measures value of molecular area of the mixed monolayer and that averaged according to the molar fraction of the mixed monolayer at the same surface pressure [40] gives positive values. This implies that sp-85 has an area-expanding effect, and indicates non-ideality of mixing [41], in agreement with the positive values of the excess free energies. This shift to higher areas is maintained both at low and high pressures, indicating that sp-85 remains strongly bound to the lipid and is not squeezed out of the monolayer at high pressures. This is also the case with other AMPs, such as PxB [29]. The mixing behavior of sp-85 with saturated DPPG and DPPE:DPPG monolayers is very similar, considering the more packed state of these monolayers of saturated lipids, and thus these monolayers where used to obtain Langmuir Blodgett films on solid support. Surface morphology images of LB films with 5% sp-85 confirm the conclusions obtained from the thermodynamic analysis of the π–area curves, with a disordering effect of lipid packing that is visible even at 32 mN m^{-1}, considered to be equivalent to the biological membrane pressure [30].

Membrane perturbation is further confirmed with liposomes of the same composition, where sp-85 causes lipid mixing and leakage of aqueous contents starting at very low concentration. Fusion and permeabilization are favored by POPE, an effect that could be related to the pronounced impact of POPE on the membrane lateral pressure profile, increasing acyl chain packing and

Please cite this article in press as: A. Grau-Campistany, et al., Membrane interaction of a new synthetic antimicrobial lipopeptide sp-85 with broad spectrum activity, Colloids Surf. A: Physicochem. Eng. Aspects (2014), http://dx.doi.org/10.1016/j.colsurfa.2014.10.062

conferring negative spontaneous curvature [34]. Another possibility is a peptide-induced demixing or phase-segregation in the PE/PG membranes, as described for cyclic arginine and tryptophan-rich peptides [42] and other peptides [43]. The resulting lipid phase boundaries may result in packing defects. Interestingly, no destabilization is observed in liposomes of zwitterionic POPC, a phospholipid that is characteristic of eukaryotic membranes. In contrast, we have previously shown that the parent peptide PxB interacts with the anionic membranes in a different way, with membrane fusion and leakage appearing only at concentrations well above the MIC of this peptide [23]. This has been discussed in the context of the selectivity of PxB for Gram negative bacteria, since PxB acts by promoting the mixing of lipids between the inner and outer membranes that form the cell wall of Gram negative bacteria [14,15]. Although sp-85 is hemolytic at high concentrations, almost no hemolysis is detected at concentrations of up to five fold its average MIC in the assayed bacteria.

In conclusion, the activity and selectivity of sp-85 are due to a fine balance of its cationic and hydrophobic nature. Electrostatic interactions are favored by the presence of two Arg residues, an aminoacid that is present in many AMPs due to its strong interaction with PG headgroups [19,20]. It is well known that the increase in hydrophobicity obtained from fatty acid acylation of AMPs increases antimicrobial activity by favoring the interaction with the lipid membrane [44]. Polymyxin B nonapeptide, a deacylated derivative of PxB, is devoid of antimicrobial activity although it can bind to the outer membrane of Gram negative bacteria [45]. Probably, the long C12 fatty acid allows the intercalation of sp-85 between the phospholipid acyl tails, thus favoring the interaction of the hydrophilic part with the anionic phospholipids, as also described for lipopeptide MSI-843 [36]. The concentration dependent and instant release of aqueous contents from POPG and POPE:POPG liposomes is shared by many AMPs and suggests lysis by either a carpet mechanism or channel formation [46,47]. The action of sp-85 on the membrane is confirmed with the observation of treated bacteria by TEM, where membranous inclusions and disruption of the cell wall in *E. coli* is seen after 120 min of exposure. Appearance of additional membrane structures has also been described in *E. coli* treated with gramicidin S [48], and has been related to the fact that the amphiphilic peptide gets embedded in the lipid bilayer, causing a significant lateral expansion of the membrane area upon binding and insertion, as also observed from the mixed isotherms of sp-85 and PG or PE/PG monolayers.

Correlating structure and function of biologically active peptides is crucial for understanding the underlying molecular and physicochemical basis of their mode of action. The data presented here provide evidence for the specificity of sp-85 for negatively charged membranes of a composition that is similar to that found in bacterial membranes. The inclusion of two residues of arginine and the longer fatty acid of this peptide has a clear effect on the interaction with the membrane, increasing the destabilization of anionic lipid membranes.

Acknowledgements

We thank Ministerio de Ciencia e Innovación (CTQ2008-06200), Generalitat de Catalunya (VAL-TEC 08-1-0016, ACC10), Xarxa de Referència en Biotecnologia and Fundació Bosch i Gimpera (UB) for supporting this work. We are very grateful to Helena Martin (University of Barcelona) and Deniz Çorba (Ege University, Turkey) for the support in monolayer experiments.

References

[1] Ch.T. Walsh, T.A. Wencewicz, Prospects for new antibiotics: a molecule-centered perspective, J. Antibiot. 67 (2014) 7–22.
[2] A.E. Aiello, E. Larson, Bacterial cleaning and hygiene products as an emerging risk factor for antibiotic resistance in the community, Lancet Infect. Dis. 3 (2003) 501–506.
[3] A.S. Fauci, Infectious diseases considerations for the 21st century, Clin. Infect. Dis. 32 (2001) 675–685.
[4] H.W. Boucher, G.H. Talbot, J.S. Bradley, J.E. Edwards, D. Gilbert, L.B. Rice, M. Scheld, B. Spellberg, J. Bartlett, Bad Bugs, No Drugs: No ESKAPE! an update from the Infectious Diseases Society of America, Clin. Infect. Dis. 48 (2009) 1–12.
[5] L.B. Rice, Antimicrobial resistance in gram-positive bacteria, Am. J. Infect. Control 34 (2006) S11–S19.
[6] G.C. Ainsworth, A.M. Brown, G. Brownlee, Aerosporin, an antibiotic produced by *Bacillus aerosporus* Greer, Nature 160 (1947) 263.
[7] D. Landman, C. Georgescu, D.A. Martin, J. Quale, Polymyxins revisited, Clin. Microbiol. Rev. 21 (2008) 449–465.
[8] J.M. Pogue, D. Marchaim, D. Kaye, Revisiting older antimicrobials in the era of multidrug resistance, Pharmacotherapy 31 (2011) 912–921.
[9] M. Zasloff, Antimicrobial peptides of multicellular organisms, Nature 415 (6870) (2002) 389–395.
[10] L.T. Nguyen, E.F. Haney, H.J. Vogel, The expanding scope of antimicrobial peptide structures and their modes of action, Trends Biotechnol. 29 (2011) 464–472.
[11] L.M. Gottler, A. Ramamoorthy, Structure, membrane orientation, mechanism, and function of pexiganan — a highly potent antimicrobial peptide designed from magainin, Biochim. Biophys. Acta 1788 (2009) 1680–1686.
[12] G. Laverty, S.P. Gorman, B.F. Gilmore, The potential of antimicrobial peptides as biocides, Int. J. Mol. Sci. 12 (2011) 6566–6596.
[13] J.T. Oh, Y. Cajal, P.S. Dhurjati, T.K. Van Dyk, M.K. Jain, Cecropins induce the hyperosmotic stress response in *Escherichia coli*, Biochim. Biophys. Acta 1415 (1998) 235–245.
[14] J.T. Oh, Y. Cajal, E.M. Skowronska, S. Belkin, J. Chen, T.K. Van Dyk, M. Sasser, M.K. Jain, Cationic peptide antimicrobials induce selective transcription of micF and osmY in *Escherichia coli*, Biochim. Biophys. Acta 1463 (2000) 43–54.
[15] J.T. Oh, T.K. Van Dyk, Y. Cajal, P.S. Dhurjati, M. Sasser, M.K. Jain, Osmotic stress in viable *Escherichia coli* as the basis for the antibiotic response by polymyxin B, Biochem. Biophys. Res. Commun. 246 (1998) 619–623.
[16] F. Rabanal, Y., Cajal, M. Garcia-Subirats, M. Rodríguez, Compuestos peptídicos antibacterianos, ES2008/02626; WO2010/029196 A1.
[17] F. Rabanal, Y., Cajal, M. García, M. Rodriguez, Compuestos peptídicos útiles como agentes antibacterianos, ES201000349, ES 2.374.779 A1, WO 2011 110716, US 2013 053305.
[18] F. Rabanal, Y., Cajal, A. Grau-Campistany, J., Vila, X. Vila, Compuestos peptídicos útiles como agentes antibióticos, P201330519, PCT/ES2014/070286, WO 2014 167160 A1.
[19] S.M. Fuchs, R.T. Raines, Internalization of cationic peptides: the road less (or more?) traveled, Cell. Mol. Life Sci. 63 (2006) 1819–1822.
[20] D.I. Chan, E.J. Prenner, H.J. Vogel, Tryptophan- and arginine-rich antimicrobial peptides: structures and mechanisms of action, Biochim. Biophys. Acta 1758 (2006) 1184–1202.
[21] R.M. Epand, S. Rotem, A. Mor, B. Berno, R.F. Epand, Bacterial membranes as predictors of antimicrobial potency, J. Am. Chem. Soc. 130 (2008) 14346–14352.
[22] F. Rabanal, J.M. Tusell, L. Sastre, M.R. Quintero, M. Cruz, D. Grillo, M. Pons, F. Albericio, J. Serratosa, E. Giralt, Structural, kinetic and cytotoxicity aspects of 12-28 β-amyloid protein fragment: a reappraisal, J. Peptide Sci. 8 (2002) 578–588.
[23] Y. Cajal, J. Ghanta, K. Easwaran, A. Surolia, M.K. Jain, Specificity for the exchange of phospholipids through polymyxin B mediated intermembrane molecular contacts, Biochemistry 35 (1996) 5684–5695.
[24] H. Ellens, J. Bentz, F.C. Szoka, H^+- and Ca^{2+}-induced fusion and destabilization of liposomes, Biochemistry 24 (1985) 3099–3106.
[25] G.L. Woods, J.A. Washington, Antibacterial susceptibility test: dilution and disk diffusion methods, in: O.R. Murray (Ed.), Manual of Clinical Microbiology, 6th ed., American Society for Microbiology, Washington, DC, 1995, pp. 1327–1341.
[26] A. Zaragoza, F.J. Aranda, M.J. Espuny, J.A. Teruel, A. Marqués, A. Manresa, A. Ortiz, Hemolytic activity of a bacterial trehalose lipid biosurfactant produced by *Rhodococcus* sp.: evidence for a colloid–osmotic mechanism, Langmuir 26 (2010) 8567–8572.
[27] J.T. Davies, E.K. Rideal, Interfacial Phenomena, 2nd ed., Academic Press, New York, 1963, pp. 265.
[28] P. Wydro, M. Flasinski, M. Broniatowski, Molecular organization of bacterial membrane lipids in mixed systems—a comprehensive monolayer study combined with grazing incidence X-ray diffraction and Brewster angle microscopy experiments, Biochem. Biophys. Acta 1818 (2012) 1745–1754.
[29] A. Clausell, M.A. Busquets, M. Pujol, M.A. Alsina, Y. Cajal, Polymyxin B-lipid interactions in Langmuir–Blodgett monolayers of *Escherichia coli* lipids: a thermodynamic and atomic force microscopy study, Biopolymers 75 (2004) 480–490.
[30] D. Marsh, Lateral pressure in membranes, Biochem. Biophys. Acta 1286 (1996) 163–223.
[31] A. Clausell, F. Rabanal, M. Garcia-Subirats, M.A. Alsina, Y. Cajal, Membrane association and contact formation by a synthetic analogue of polymyxin B and its fluorescent derivatives, J. Phys. Chem. B 110 (2006) 4465–4471.
[32] C. Ege, K.Y.C. Lee, Insertion of Alzheimer's Aβ40 peptide into lipid monolayers, Biophys. J. 87 (2004) 1732–1740.
[33] L. Zhang, Interaction of cationic antimicrobial peptides with model membranes, J. Biol. Chem. 276 (2001) 35714–35722.
[34] H. Zhao, R. Sood, A. Jutila, S. Bose, G. Fimland, J. Nissen-Meyer, P.K.J. Kinnunen, Interaction of the antimicrobial peptide pheromone plantaricin A with model

membranes: implications for a novel mechanism of action, Biochim. Biophys. Acta 1758 (2006) 1461–1474.
[35] E. Rubinchik, T. Schneider, M. Elliott, W.R.P. Scott, J. Pan, C. Anklin, H. Yang, D. Dugourd, A. Müller, K. Gries, S.K. Straus, H.G. Sahl, R.E.W. Hancock, Mechanism of action and limited cross-resistance of new lipopeptide MX-2401, Antimicrob. Agents Chemother. 55 (2011) 2743–2754.
[36] S. Thennarasu, D.-K. Lee, A. Tan, U.P. Kari, A. Ramamoorthy, Antimicrobial activity and membrane selective interactions of a synthetic lipopeptide MSI-843, Biochim. Biophys. Acta 1711 (2005) 49–58.
[37] M. Wenzela, A.I. Chiriacb, A. Ottoc, D. Zweytickd, C. Maye, C. Schumacherf, R. Gustg, H.B. Albadah, M. Penkovah, U. Krämeri, R. Erdmannj, N. Metzler-Nolteh, S.K. Strausk, E. Bremerl, D. Becherc, H. Brötz-Oesterheltf, H.-G. Sahlb, J.E. Bandow, Small cationic antimicrobial peptides delocalize peripheral membrane proteins, Proc. Natl. Acad. Sci. U.S.A. 111 (2014) E1409–E1418.
[38] E. Sevcsik, G. Pabst, W. Richter, S. Danner, H. Amenitsch, K. Lohner, Interaction of LL-37 with model membrane systems of different complexity: influence of the lipid matrix, Biophys. J. 94 (2008) 4688–4699.
[39] R. Maget-Dana, The monolayer technique: a potent tool for studying the interfacial properties of antimicrobial and membrane-lytic peptides and their interactions with lipid membranes, Biochim. Biophys. Acta 1462 (1999) 109–140.
[40] I.S. Costin, G.T. Barnes, Two-component monolayers. II. Surface pressure–area relations for the octadecanol–docosyl sulphate system, J. Colloid Interface Sci. 51 (1975) 106–121.
[41] A. Chávez, M. Pujol, I. Haro, M.A. Alsina, Y. Cajal, Membrane fusion by an RGD-containing sequence from the core protein VP3 of hepatitis A virus and the RGA-analogue: implications for viral infection, Biopolymers 58 (2001) 63–77.
[42] Ch. Junkes, R.D. Harvey, K.D. Bruce, R. Dölling, M. Bagheri, M. Dathe, Cyclic antimicrobial R-, W-rich peptides: the role of peptide structure and *E. coli* outer and inner membranes in activity and the mode of action, Eur. Biophys. J. 40 (2011) 515–528.
[43] K. Lohner, E. Sevcsik, G. Pabst, Liposome-based biomembrane mimetic systems: implications for lipid–peptide interactions, Adv. Planar Lipid Bilayers Liposomes 6 (2008) 103–137.
[44] D. Avrahami, Y. Shai, Bestowing antifungal and antibacterial activities by lipophilic acid conjugation to D,L-amino acid-containing antimicrobial peptides: a plausible mode of action, Biochemistry 42 (2003) 14946–14956.
[45] A. Rustici, et al., Molecular mapping and detoxification of the lipid A binding site by synthetic peptides, Science 259 (1993) 361–364.
[46] V. Balhara, R. Schmidt, S.-U. Gorr, Ch. DeWolf, Membrane selectivity and biophysical studies of the antimicrobial peptide GL13K, Biochim. Biophys. Acta 1828 (2013) 2193–2203.
[47] J. Sun, Y. Xia, D. Li, Q. Du, D. Liang, Relationship between peptide structure and antimicrobial activity as studied by *de novo* designed peptides, Biochim. Biophys. Acta 1838 (2014) 2985–2993.
[48] M. Hartmann, M. Berditsch, J. Hawecker, M.F. Ardakani, D. Gerthsen, A. Ulrich, Damage of the bacterial cell envelope by antimicrobial peptides gramicidin S and PGLa as revealed by transmission and scanning electron microscopy, Antimicrob. Agents Chemother. 54 (2010) 3132–3142.

Please cite this article in press as: A. Grau-Campistany, et al., Membrane interaction of a new synthetic antimicrobial lipopeptide sp-85 with broad spectrum activity, Colloids Surf. A: Physicochem. Eng. Aspects (2014), http://dx.doi.org/10.1016/j.colsurfa.2014.10.062